Chinese Chemical Letters 33 (2022) 4191–4196

Contents lists available at ScienceDirect

Chinese Chemical Letters

journal homepage: www.elsevier.com/locate/cclet

# Liposome-based anchoring and core-encapsulation for combinatorial cancer therapy

Qingqing Xiao[1], Xiaotong Li[1], Chang Liu, Yi Yang, Yuqi Hou, Ying Wang, Mengxiang Su*, Wei He*

*School of Pharmacy, China Pharmaceutical University, Nanjing 211198, China*

ARTICLE INFO

*Article history:*
Received 15 November 2021
Revised 20 January 2022
Accepted 27 January 2022
Available online 3 February 2022

*Keyword:*
Liposomes
Co-delivery
Chemotherapy
Pro-apoptotic protein
Tumor targeting

ABSTRACT

Downregulated pro-apoptotic protein in cancer cells compromises the chemotherapy by a cytotoxic drug. Here, we report co-delivery of a pro-apoptotic protein, caspase 3 (Cas 3), and cytotoxic agent, oridonin (ORD), for synergistic cancer treatment, using a method of liposome-based anchoring and core encapsulation. First, ORD is modified with hyaluronic acid (HA) to improve its solubility. Then, the targeted co-delivery system is prepared by assembling the conjugate HA-ORD onto the Cas 3-loaded liposomes, which the surface HA can target the CD44 receptor on cancer cells. *In vitro*, the co-loaded liposomes (120 nm) are specifically taken up by 4T1 cells and endow a 1.5-fold increase of Cas 3. After intravenous injection into the tumor-bearing mice, the liposomes accumulate in the tumor with high efficacy and significantly inhibit tumor growth via promoting apoptosis and anti-proliferation of cancer cells. Mechanistically, the co-delivery works synergistically by upregulating the activated Cas form, cleaved-Cas 3.



Breast cancer was the most commonly diagnosed cancer globally, accompanying approximately 2.26 million cases [1]. The cancer occurrence mainly results from cell apoptosis disorder, which inhibits pro-apoptotic signals in tumor cells while anti-apoptotic proteins are upregulated. Two initiation pathways are frequently involved in cell apoptosis: activating death receptors through external damage and triggering the release of cytochrome c and other substances from the mitochondria via intrinsic pathways [2]. Clinical evidence shows that the combination of traditional chemotherapy and pro-apoptotic agents can synergistically elevate the survival rate of cancer patients [3]. Furthermore, caspase 3 (Cas 3) is a significant mediator of cancer cell apoptosis after exposure to cytotoxic drugs or radiotherapy [4,5]. Therefore, we theorized that combinatorial use of Cas 3 and the cytotoxic drug could represent a promising regimen to combat cancer.

Poor drug delivery to the tumor site is a significant limitation that hinders cancer treatment. Drug carriers can improve tumor targeting because of their small size and penetration inside the diseased area [6]. Liposomes (Lips) are enclosed spherical vesicles composed of one or more lipid bilayers [7]. Lips are emerging as promising carriers to enhance drug delivery due to the advantages, including high payload capacity, prolonged blood circulation time, targeting ability to the disease site, and ignorable toxicity to the body [8–10]. Over 20 liposomal formulations were approved for clinical use [11]. In this study, we co-delivered oridinon (ORD) and Cas 3 using Lips for the combined treatment of breast cancer in 4T1 tumor-bearing mice. ORD is a natural compound with poor solubility isolated from the traditional Chinese medicine Rubescenin [12]. It has a robust ability to fight against various cancers such as liver cancer, prostate cancer, and breast cancer [13–17]. Briefly, ORD was conjugated with hyaluronic acid (HA) to improve its solubility. After that, the co-delivery system, hybrid nanoparticles (HNPs), was prepared by assembling the HA-ORD conjugate onto the Cas 3-loaded liposomes, which the conjugate hydrophobic segment anchored into the liposomal membrane and, meanwhile, the HA part located on the HNPs surface to target CD44 receptor on cancer cells (Scheme 1) [18,19]. The targeted co-delivery system efficiently accumulated in the tumor and inhibited the tumor growth synergistically through upregulation of the activated Cas 3 form, cleaved-Cas 3.

First, the conjugate HA-ORD was synthesized *via* esterification reaction as described in previous report [20]. Cas 3-Lips were prepared by the reverse-phase evaporation method [21]. As depicted in Table S1 (Supporting information), the protein-encapsulated Lips have a diameter of 120 nm and a protein encapsulation efficacy (EE) of greater than 50% in the formulations with protein/lipid ratios (w/w) of 1:10–1:30. The protein encapsulation was identified by SDS-PAGE, in which the demulsification separated protein bands

* Corresponding authors.
*E-mail addresses:* sumengxiang@cpu.edu.cn (M. Su), weihe@cpu.edu.cn (W. He).
[1] These author contributed equally to this work.

https://doi.org/10.1016/j.cclet.2022.01.083
1001-8417/

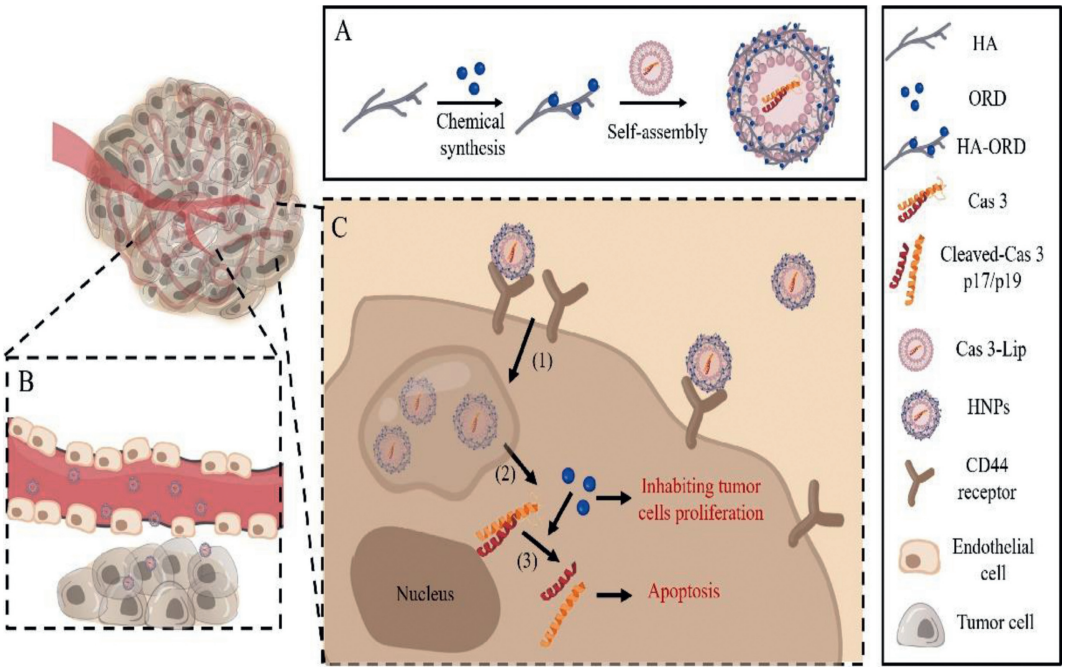


**Scheme 1.** (A) Preparing the co-delivery system (HNPs) by anchoring the conjugate HA-ORD onto Cas 3-Lips. (B and C) Purposed performance *in vivo*. After intravenous injection, (B) HNPs accumulate in the tumor, and (C-1) target tumor cells through CD44-HA receptor-ligand interaction, (C-2) release the two active ingredients inside the cells, and (C-3) synergistically activate Cas-3 pathway to promote apoptosis of tumor cells.

significantly weakened compared with the control (Fig. 1A). The protein/lipid ratios had a modest influence on the diameter and EE; however, the ratio increase reduced the drug-loading capacity from approximately 5% to 2%. Accordingly, the Lip formulation with a protein/lipid ratio of 1:10 was selected for further study due to its highest drug payload. Then, the co-delivery system, HA-ORD/Cas 3-Lip HNPs, was prepared by assembling the conjugate onto the Cas 3-Lips. The particle size of HNPs increased from 113 nm to 274 nm with a gradual decrease in the zeta potential as HA/lipid ratio elevated from 1:4 to 2:1 (w/w) (Table S2 in Supporting information). To investigate the co-assembly, we conducted the FRET study for the HNPs with various HA/lipid mass ratios by using FITC as a donor conjugated with HA-ORD and Rho as the acceptor encapsulated in the Lips. With the increase of Rho-Lips in the HNPs, the maximal fluorescence intensity of the acceptor (Rho) at 575 nm increased significantly. In comparison, the maximal fluorescence intensity of the donor (FITC) at 515 nm decreased, indicating the FRET occurrence (Fig. 1B). FRET is a potent tool for studying the interaction between two materials by labeling fluorescent donor and acceptor [22–24]. Consequently, the assembly of the conjugate and the Lips was confirmed.

The HNPs with the HA/lipid ratio of 1:2 were selected for further study due to the smaller diameter (~118 nm) and higher loading of Cas 3. TEM test displayed that the Lips and HNPs had spherical morphology (Fig. 1C). The drug EE% and DL% in total in HNPs was 48.75% and 7.92%, respectively, which the DL% of Cas 3 and ORD was 4.75% and 3.17%, respectively. Incubation in 10% serum for 12 h imposed a slight alteration in diameter, surface charge, and morphology of the two nanoparticles (Figs. 1D–F). However, their PDI and surface potential gradually increased during the incubation period of 12–24 h. It is worth noting that these increase from HNPs was compromised compared with Lips. The data demonstrated that the conjugate assembly could improve the serum stability of Lips. Release study shows that 60%–80% of encapsulated dye carboxyfluorescence (CF) in the core of liposomes from HNPs was released at 2 h under different pH conditions (Fig. 1G), indicating that HNPs can effectively release the encapsulated drug. Meanwhile, the HA-ORD release from HNPs was pH-dependent, increasing pH value resulting in a faster release. Interestingly, the release at pH 5 was significantly slower than at pH 6.8 and 7.4. The profile demonstrated that the conjugate has an elevated force to anchor onto liposome under low pH conditions and might help maintain the structural stability of HNPs in the acidic tumor microenvironment (Fig. 1H).

Next, the uptake study in 4T1 cells was performed by flow cytometry. As displayed in Figs. S1 and S2 (Supporting information), the uptake of the conjugate and the two nanoparticles was time-dependent in a specific period. Especially, HNPs reached their maximal uptake at 1 h after incubation, while Lips did not get the most significant uptake at even 4 h (Fig. S1B), indicating faster endocytosis of HNPs. The further experiment showed that the uptake of HNPs was concentration-dependent (Figs. S1C and D).

The CD44 receptor is overexpressed on various tumor cells [25], and HA is a specific ligand for CD44 [26–28]. To verify CD44 role in HNPs uptake, we saturated the surface CD44 receptors by pre-incubating 4T1 cells with excess free HA. Flow cytometry assay showed that Rho-HNPs uptake in the pretreated cells was significantly reduced compared with unsaturated cells ($P < 0.05$, Fig. S1E). Laser scanning confocal microscope (CLSM) observation indicated HA pretreatment resulted in weaker intracellular fluorescence intensity (Fig. S1F). To further prove the targetability of HNPs to cancer cells, we investigated the uptake in 4T1 cells and the control cell line without over-expressing CD44 receptors, NIH 3T3. As expected, the uptake of HNPs in 4T1 cells was significantly higher than that in NIH 3T3 cells under fixed FITC or Rho concentration conditions (Figs. S1G and H). These results confirmed that the conjugate anchoring promoted the Lips uptake in tumor cells through the specific HA/CD44 ligand/receptor affinity.

To test the anti-tumor activity, we incubated preparations with 4T1 cells. Cas 3-Lips display improved cytotoxicity to 4T1 cells at the protein concentrations of ≥ 2.5 μg/mL compared with free Cas 3 (Fig. S3A in Supporting information), owing to that liposome encapsulation can improve the protein stability and promote the uptake. The conjugate HA-ORD had concentration-dependent cytotoxicity. The ORD in the conjugate could be released due to the

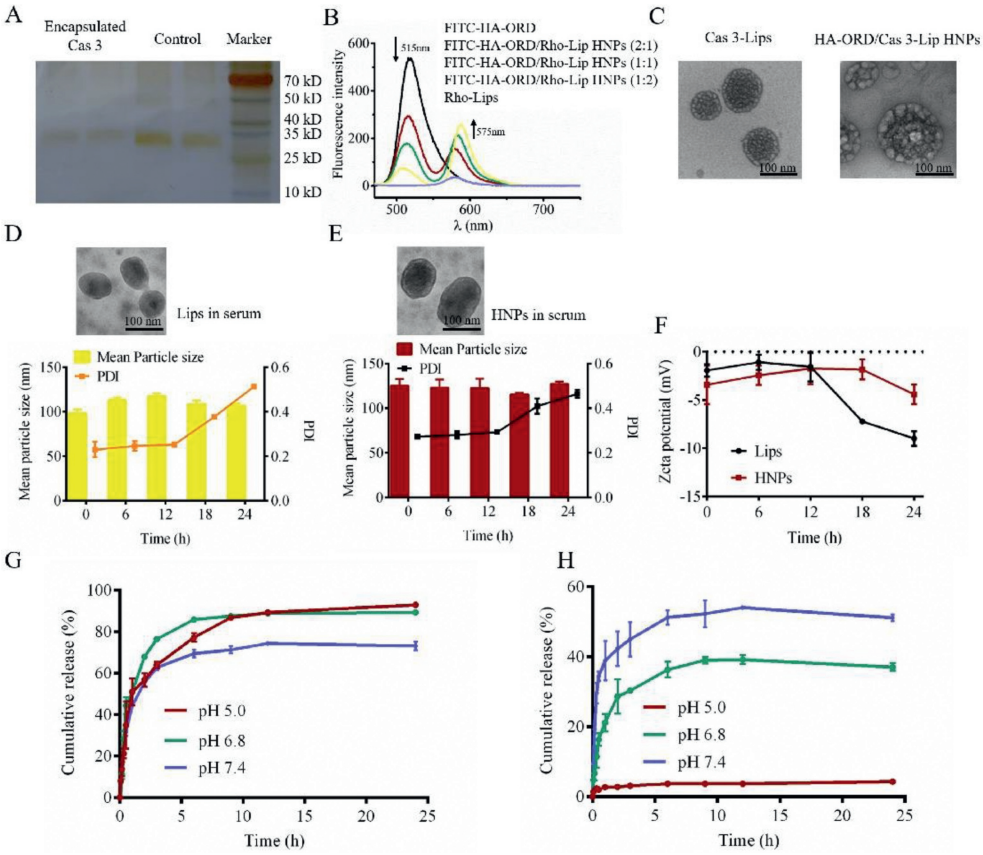


**Fig. 1.** Characterization: (A) SDS PAGE of free Cas 3 and separated Cas 3 after Cas 3-Lips demulsification. (B) Fluorescence emission spectra of FITC-HA-ORD, Rho-Lips and FITC-HA-ORD/Rho-Lip HNPs with various HA/lipid mass ratios. $\lambda_{ex} = 450$ nm. (C) TEM images of Cas 3-Lips and HA-ORD/Cas 3-Lip HNPs. The scale bar is 100 nm. (D and E) Serum stability of Lips and HNPs in 10% FBS at 37 °C. The change of the (D, E) morphology, size, PDI, and (F) $\zeta$-potential of Lips and HNPs. (G) *In vitro* release of CF from CF-labeled HNPs at 37 °C. CF was encapsulated in the cores of HNPs. (H) *In vitro* release of FITC-HA-ORD from HNPs. Data are presented as mean ± SD ($n = 3$). The samples collected at specified time intervals were placed in a 96-well plate to measure fluorescence intensity using a fluorescence spectrometer (CF, $\lambda_{ex} = 492$ nm and $\lambda_{em} = 515$ nm; FITC, $\lambda_{ex} = 490$ nm and $\lambda_{em} = 520$ nm).

ester-bond degradation by the cytosol esterase [29]. Therefore, the conjugate HA-ORD demonstrated toxicity against cancer cells. In contrast, HNPs showed the most profound cytotoxicity among the preparations at specific drug concentrations (31.3 μg/mL, Fig. S3B in Supporting information), accompanied with a 2-fold cytotoxicity increase in contrast with the simple combination of Cas 3 and the conjugate.

The synergy effect was investigated by measuring the cytotoxicity of HNPs with different mass ratios of HA/lipid (2:1, 1:1, 1:2, 1:4) and calculating the combination index (CI) by Compusyn software. The CI values from formulations with ratios of 2:1, 1:1, 1:2 are <1 at a specific low inhibition rate (Fa), while, at all Fa, the CI from 1:4 ratio is not great than 1 (Figs. S3C and D in Supporting information), indicating its improved synergy. As a result, the HNPs with HA/lipid of 1:4 were selected for further study.

Apoptosis determination displayed that HA-ORD and Cas-Lips had 60% and 10% of 4T1 cell apoptosis after 48 h incubation. However, the simple combination formulation did not lift the apoptosis rate (60%) compared with HA-ORD. In contrast, HNPs exhibited an 83% apoptosis rate and thus indicated the co-delivery allowed enhanced apoptosis of cancer cells (Figs. S3E and F in Supporting information).

Then, the level of critical proteins in the apoptosis process was determined by WB. Cas 3 exists in an inactive precursor form in cells. After being activated, it is cleaved at an aspartate and is broken down into cleaved-Cas 3 [30]. Finally, cleaved-Cas 3 initiates the downstream protein pathway or blocks DNA repair to induce cell apoptosis [31–33]. Therefore, we determined the expression level of Cas 3 and cleaved-Cas 3 after preparation incubation. As depicted in Fig. 2, the dosing with HNPs endorsed the highest level of Cas 3 and cleaved-Cas 3 in tumor cells, verifying the intracellular delivery of Cas 3 and its activation. Also, the conjugate induced Cas 3 expression and implied its potential ability to promote tumor cell apoptosis.

To study the biodistribution, we labeled fluorescence probe DiR (DiIC 18 (7); 1,1′-dioctadecyl-3,3,3′,3′-tetramethylindotricarbocyanine iodide) to the nanoparticles for imaging [34]. After intravenous injection, *in vivo* imaging of 4T1 tumor-bearing mice at specific time points was executed. Both DiR-Lips and DiR-labeled HNPs effectively accumulated at the tumor site for 24 h period compared with free DiR (Fig. 3). Whereas the tumor accumulation of DiR-labeled HNPs, especially at 24 h post-injection, was greater than that of DiR-Lips ($P < 0.05$, Fig. 3C). *Ex vivo* imaging for separated major tissues collected at 24 h further verified that DiR-labeled HNPs had improved tumor-targeting ability over DiR-Lips (Fig. 3B). These results indicated that the conjugate anchoring promoted the tumor accumulation of Lips and prolonged the residence time.

To study the anti-tumor efficacy, we intravenously administered different preparations to 4T1 tumor-bearing mice every 3 days for 5 doses in 18 days. The tumor volume at 18 days in the saline- or free Cas 3-treated group increased by >10-fold compared to that at 0 day, while the tumor volumes in the group treated with HA-ORD group or the physical mixture (free Cas 3 plus HA-ORD)

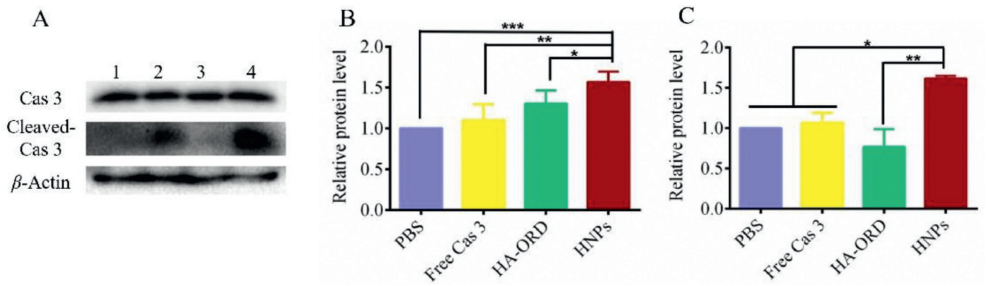


**Fig. 2.** Expression of the pro-apoptotic protein in 4T1 cells: (A) WB analysis of Cas 3 and cleaved-Cas 3 expressions in cells after treatment with preparation for 48 h at an ORD concentration of 0.5 mg/mL or Cas 3 concentration of 10 μg/mL. β-Actin was used as a loading control. Dark bands indicate protein expression. Quantitative analysis of the expression of (B) Cas 3 and (C) cleaved-Cas 3. mean ± SD, $n = 3$, $^{*}P < 0.05$, $^{**}P < 0.01$, $^{***}P < 0.001$. Preparations: 1, saline; 2, free Cas 3; 3, HA-ORD; 4, HNPs.

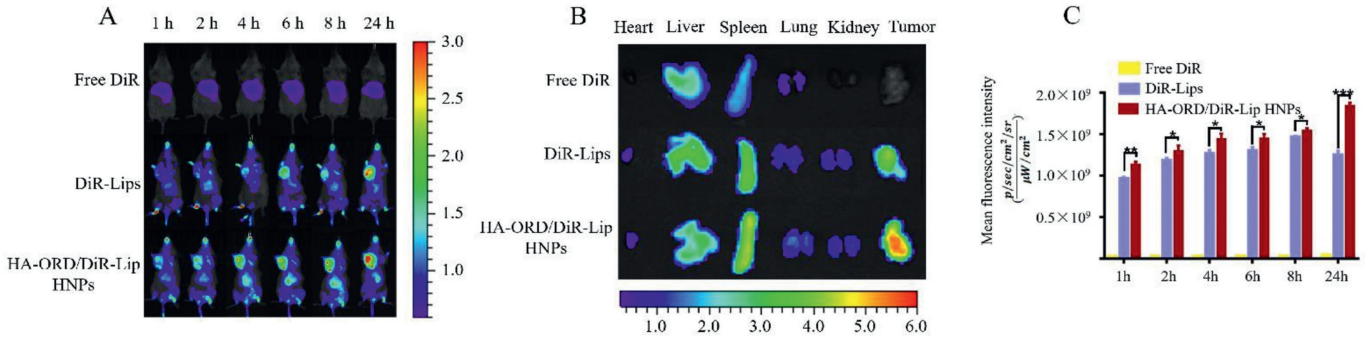


**Fig. 3.** Tumor targeting *in vivo*: (A) *In vivo* fluorescence imaging of 4T1 tumor-bearing mice after i.v. injection of DiR-labeled preparations at the dye dose of 0.5 mg/kg, according to the body weight. (B) *Ex vivo* fluorescence images of important tissues were collected at 24 h post-injection. (C) Quantitative analysis of tumor accumulation at different time points ($n = 3$, $^{*}P < 0.05$, $^{**}P < 0.01$).

group has 7-fold growth. Significantly, the tumor volume from the groups dosed with HNPs at low or high does exhibited a 5-fold increase and demonstrated significant tumor growth inhibition (Fig. 4A). The animal's body weight in all groups did not decline and, instead, increased at a steady rate (Fig. 4B). These results indicated that HA-ORD and HNPs safely regressed the tumor growth in 4T1 tumor-bearing mice, whereas HNPs had improved inhibition.

The cancer-cell apoptosis in the isolated tumors was examined by TUNEL and Ki67 assay [35]. Positive cells shown in TUNEL-stained sections were most profound in the groups treated with high or low doses of HNPs, followed by the groups treated with preparations containing HA-ORD (Fig. S4 in Supporting information). Quantified determination displayed that HNPs treatment allowed a 50% apoptosis rate in the tumor cell, 5 folds as great as saline treatment. The apoptosis rate of the two groups dosed with preparations containing HA-ORD, HA-ORD, and physical mixture, reached 30% as well (Fig. 4C). The apoptosis result was confirmed by the anti-proliferation determination by Ki67 assay (Fig. 4D and Fig. S4). The H&E staining assay further demonstrated that the fewest cell numbers were observed in the tumor treated with HNPs (Fig. S4).

We hypothesized that the tumor-suppressor effect of HNPs was directly related to the delivery and activation of Cas 3. Accordingly, the protein in the isolated tumors was determined by WB assay. Administration with low dose HNPs increased the Cas 3 level by 50% compared with treatment with other preparations ($P < 0.05$, Figs. 4E and F). Moreover, the activated Cas 3 form, cleaved-Cas 3, in the group dosed with low dose HNPs raised by approximately 2 folds compared to that from the saline-treated group ($P < 0.001$, Figs. 4E and G). The results indicated that the HNPs could effectively deliver Cas 3 into the tumor.

Overall, HNPs played a significant therapeutic role in the 4T1 breast cancer model by inhibiting tumor growth and promoting tumor cell apoptosis.

In this study, we demonstrated that the liposome-anchored strategy was promising to promote the co-delivery of active components with high molecular weight. Co-delivery of small molecular drugs using drug carriers has obtained breakthroughs, as evident by the approval of Vyxeos liposomes co-loading daunorubicin and cytarabine to treat acute myeloid leukemia in 2017 [36]. However, co-delivery of two molecules with a high molecular weight with carriers is still a considerable challenge due to their limited space for loading. To enlarge the loading space, researchers incorporated cationic materials, such as polyethyleneimine (PEI) and dioleoyl phosphatidyl ethanolamine, into the liposomes to condense the second macromolecular drug on the surface [37]. Nonetheless, their incorporation often induces significant toxicity to the body and hinders the translation of the co-delivery system. Herein, we found that the strategy of liposome-based anchoring and core encapsulation enabled the co-delivery of the two active molecules without additional cationic materials. The functional protein was encapsulated in the core of liposomes and whereas the second drug-polymer macromolecule was anchored onto the liposomes via inserting the hydrophobic groups inside the lipid membrane. As well known, most drug-polymer or antibody-drug conjugate has hydrophobic side or residues on their structure [38]. Consequently, we believe the current approach is a universal platform to co-deliver polymer-based conjugate/prodrug and biopharmaceuticals.

The anchoring allowed the liposomes to have enhanced targeting ability to the tumor (Fig. 3). HA-ORD-anchored liposomes possessed a 50% increase of tumor accumulation over the liposomes. The profound tumor accumulation is mainly ascribed to the ligand/receptor affinity of HA/CD44 that allowed HNPs to target the tumor tissue *via* potentially overcoming the shear forces of blood flow [39,40]. Moreover, the conjugate anchoring led to an increase in the negative charge of Lips (Table S2 in Supporting information) and, as a result, could potentially reduce the adhesion of

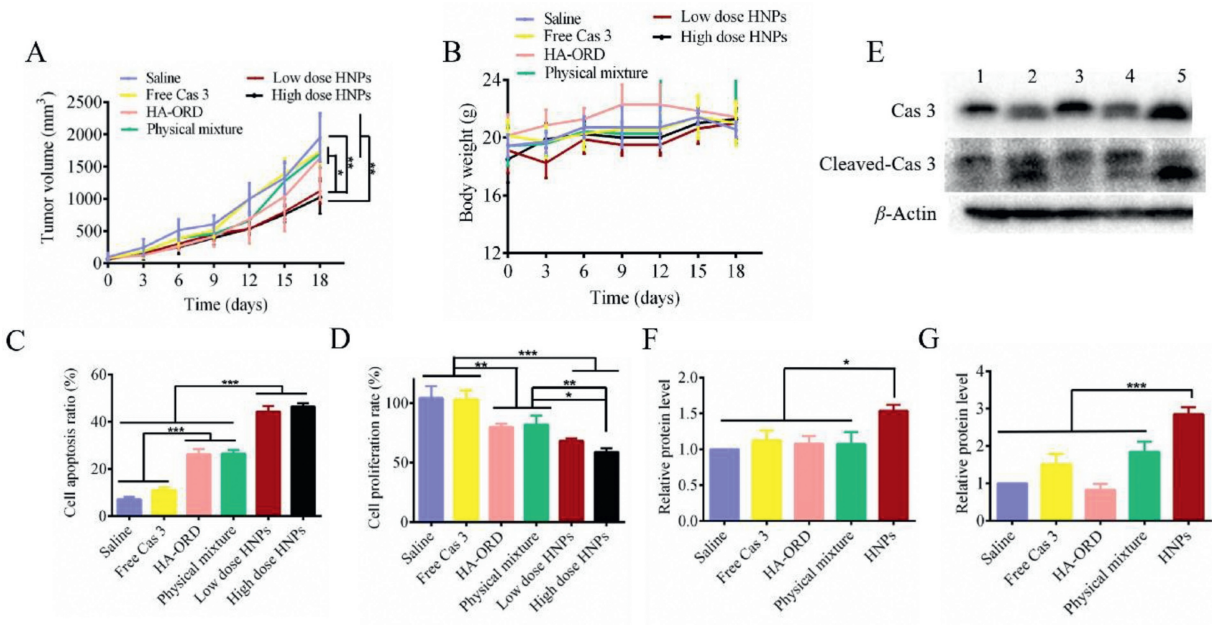


**Fig. 4.** *In vivo* anti-tumor activity: (A) Tumor-volume growth curves and (B) body-weight change profiles of 4T1 tumor-bearing mice (mean ± SD, $n = 7$). Quantitative analysis of (C) apoptosis and (D) proliferation of tumor cells (mean ± SD, $n = 3$). (E) Western blot analysis of Cas 3 and cleaved-Cas 3 expression in the isolated tumors. Preparations: 1, saline; 2, free Cas 3; 3, HA-ORD; 4, physical mixture of Cas 3 and HA-ORD; 5, HNPs. $\beta$-Actin was used as a loading control. Dark bands indicate protein expression. Quantified expression of (F) Cas 3 and (G) cleaved-Cas 3 (mean ± SD, $n = 3$). The preparations (0.2 mL) were injected to 4T1 tumor-bearing mice *via* tail veins every 3 days at an ORD dose of 5 mg/kg or a Cas 3 dose of 150 μg/kg, according to the body weight. HNPs were administrated at two doses of ORD/Cas 3, 5 mg/150 μg/kg, and 7.5 mg/225 μg/kg. $^{*}P < 0.05$, $^{**}P < 0.01$, $^{***}P < 0.001$.

blood proteins to nanoparticles, thereby protecting the nanoparticles from excessive exposure to blood proteins and extending the circulation time [41]. Third, the congruence principle might also contribute to the tumor accumulation because HNPs have rich HA on their surface, while a large HA matrix distributes in the tumor.

Various approaches were employed to improve the stability and performance of liposomes *in vitro* and *in vivo*, including nanoparticle-coating [42], polymer-stabilization by covalently linking a polymer to the head groups of lipids [43], and embedding liposomes inside another nanodevice [44]. These reported strategies either impaired the biocompatibility of liposomes or limited their translation due to the complicated preparation process. A previous report indicated that the surface coating could reduce the membrane fluidity of liposomes and enhance liposome stability *in vivo* [45]. The conjugate anchoring might decrease the membrane fluidity of liposomes as well. Consequently, our HA-based anchoring represents a promising strategy to improve the use of liposomes as drug carriers.

Co-delivery of Cas 3 and ORD is promising to inhibit tumor growth. Cas 3 is the final apoptosis executor of cancer cells and is downregulated, which has become one critical restriction for chemotherapy in cancer treatment [46,47]. Though the two therapeutics are entirely different in water solubility, molecular weight, and stability, the developed HNPs could co-load the Cas 3 and the cytotoxic ORD and precisely deliver them to cancer cells. The results displayed that the two therapeutics worked synergistically to combat cancer. The study offers a route to improve chemotherapy.

In summary, a liposome-based anchoring and core encapsulation strategy enables targeted co-delivery of two therapeutics, the conjugate HA-ORD and Cas 3, to the tumor, allowing efficient anti-tumor activities by suppressing tumor growth and enhancing apoptosis of tumor cells. Moreover, the conjugate anchoring confers positively targeting ability on liposomes, expands their drug-loading capacity, and provides the potential to facilitate the utilization of liposomes as drug carriers.

## Declaration of competing interest

There are no conflicts to declare.

## Acknowledgments

This work was supported by the National Natural Science Foundation of China (Nos. 81872823, 81872833 and 82073782), the Double First-Class (No. CPU2018PZQ13) of the CPU, the Shanghai Science and Technology Committee (No. 19430741500), the Key Laboratory of Modern Chinese Medicine Preparation of Ministry of Education of Jiangxi University of Traditional Chinese Medicine (No. zdsys-202103).

## Supplementary materials

Supplementary material associated with this article can be found, in the online version, at doi:10.1016/j.cclet.2022.01.083.

## References

[1] J. Ferlay, M. Colombet, I. Soerjomataram, et al., Int. J. Cancer 149 (2021) 778–789.
[2] M.O. Hengartner, Nature 407 (2000) 770–776.
[3] Y. Zhao, N.R. Foster, J.P. Meyers, et al., J. Thorac. Oncol. 10 (2015) 172–180.
[4] A.G. Porter, R.U. Jänicke, Cell Death Differ. 6 (1999) 99–104.
[5] P. Yadav, R. Yadav, S. Jain, A. Vaidya, Chem. Biol. Drug Des. 98 (2021) 144–165.
[6] J. Hu, X. Yuan, F. Wang, et al., Chin. Chem. Lett. 32 (2021) 1341–1347.
[7] H. He, Y. Lu, J. Qi, et al., Acta Pharm. Sin. B 9 (2019) 36–48.
[8] K.T. Magar, G.F. Boafo, X. Li, Z. Chen, W. He, Chin. Chem. Lett. 33 (2022) 587–596.
[9] Z. Shi, Q. Li, L. Mei, Chin. Chem. Lett. 31 (2020) 1345–1356.
[10] X. Wang, I.S. Mohammad, L. Fan, et al., Acta Pharm. Sin. B 11 (2021) 2585–2604.
[11] J. Di, F. Xie, Y. Xu, Adv. Drug Deliv. Rev. 154-155 (2020) 151–162.
[12] S. Wang, Z. Zhong, J. Wan, et al., Am. J. Chin. Med. 41 (2013) 177–196.
[13] S. Cao, Y. Huang, Q. Zhang, et al., Apoptosis 24 (2019) 33–45.
[14] S. Chen, J. Gao, H.D. Halicka, et al., Int. J. Oncol. 26 (2005) 579–588.
[15] T. Fujita, Y. Takeda, S. Han-dong, et al., Planta Med. 54 (1988) 414–417.
[16] T. Ikezoe, S.S. Chen, X.J. Tong, et al., Int. J. Oncol. 23 (2003) 1187–1193.
[17] S. Xia, X. Zhang, C. Li, H. Guan, Saudi Pharm. J. 25 (2017) 638–643.

[18] Z. Luo, Y. Dai, H. Gao, Acta Pharm. Sin. B 9 (2019) 1099–1112.
[19] M. Zhang, S. Gao, D. Yang, et al., Acta Pharm. Sin. B 11 (2021) 2265–2285.
[20] D. Luo, Y. Yi, K. Peng, et al., Eur. J. Med. Chem. 178 (2019) 365–379.
[21] F. Szoka, D. Papahadjopoulos, Proc. Natl. Acad. Sci. U. S. A. 75 (1978) 4194–4198.
[22] R.M. Clegg, Curr. Opin. Biotechnol. 6 (1995) 103–110.
[23] E.A. Jares-Erijman, T.M. Jovin, Nat. Biotechnol. 21 (2003) 1387–1395.
[24] W. Liu, D. Li, Z. Dong, et al., Int. J. Pharm. 587 (2020) 119682.
[25] D. Naor, S. Nedvetzki, I. Golan, L. Melnik, Y. Faitelson, Crit. Rev. Clin. Lab. Sci. 39 (2002) 527–579.
[26] A. Cadete, M.J. Alonso, Nanomedicine 11 (2016) 2341–2357.
[27] E. Karousou, S. Misra, S. Ghatak, et al., Matrix Biol. 59 (2017) 3–22.
[28] A. Spadea, J.M. Rios de la Rosa, A. Tirella, et al., Mol. Pharm. 16 (2019) 2481–2493.
[29] H. Zhang, J. Wang, W. Mao, et al., J. Control. Release 166 (2013) 147–158.
[30] N. O'Donovan, J. Crown, H. Stunell, et al., Clin. Cancer Res. 9 (2003) 738–742.
[31] D.C. Altieri, Oncogene 22 (2003) 8581–8589.
[32] X. Liu, S. Jiang, X. Tian, Y. Jiang, Int. J. Clin. Exp. Pathol. 11 (2018) 4363.
[33] T. Vántus, D. Vertommen, X. Saelens, et al., Cell. Signal. 16 (2004) 703–709.
[34] C. Teng, C. Lin, F. Huang, et al., Acta Pharm. Sin. B 10 (2020) 1521–1533.
[35] X. Du, Y. Hou, J. Huang, et al., Acta Pharm. Sin. B 11 (2021) 3272–3285.
[36] A.C. Krauss, X. Gao, L. Li, et al., Clin. Cancer Res. 25 (2019) 2685–2690.
[37] Y.F. Wang, Q.S. Wu, J.D. Wang, et al., J. Control. Release 320 (2020) 457–468.
[38] W. Yu, M. Shevtsov, X. Chen, H. Gao, Chin. Chem. Lett. 31 (2020) 1366–1374.
[39] S. Martin, H. Wang, T. Rathke, et al., Polymer 102 (2016) 342–349.
[40] M. Milinkovic, J.H. Antin, C.A. Hergrueter, C.B. Underhill, R. Sackstein, Blood 103 (2004) 740–742.
[41] K. Greish, G. Thiagarajan, H. Herd, et al., Nanotoxicology 6 (2012) 713–723.
[42] L.F. Zhang, S. Granick, Nano Lett. 6 (2006) 694–698.
[43] G.T. Qin, Z. Li, R.M. Xia, et al., Nanotechnology 22 (2011) 155605.
[44] Z.J. Chen, S.C. Yang, X.L. Liu, et al., Nano Lett. 20 (2020) 4177–4187.
[45] Y. Lv, C. Xu, X. Zhao, et al., ACS Nano 12 (2018) 1519–1536.
[46] E. Devarajan, A.A. Sahin, J.S. Chen, et al., Oncogene 21 (2002) 8843–8851.
[47] R.N. Winter, A. Kramer, A. Borkowski, N. Kyprianou, Cancer Res. 61 (2001) 1227.